Study of Sc^{41} Levels by the $Ca^{40}(p,\gamma)Sc^{41}$ Reaction*

D. H. YOUNGBLOOD,† B. H. WILDENTHAL,‡ AND C. M. CLASS
T. W. Bonner Nuclear Laboratories, Rice University, Houston, Texas
(Received 17 November 1967)

The level structure of Sc^{41} produced in the $Ca^{40}(p,\gamma)Sc^{41}$ reaction has been studied by measuring the positron activity [$E_{max}(\beta^+)=5.5$ MeV, $\tau_{1/2}=0.6$ sec] of the product nucleus. The measurements covered the range $0.6\leq E_p\leq 5.2$ MeV with a resolution width of about 5 keV. Forty-six resonances in the yield function were identified with states of Sc^{41}. Absolute yields were also measured for each resonance with a β detector of calibrated efficiency. Since all excited states of Sc^{41} are proton-unstable, these yields were attributed to transitions from the capture levels directly to the ground state. On this basis, and by assuming $\Gamma_\gamma<\Gamma_p$, values of the quantity $g\Gamma_{\gamma g.s.}$ were determined for the ground-state transition from each level. By evaluating the statistical factor g for various assumed values of the spin J, the radiative widths Γ_γ were obtained. When expressed in Weisskopf single-particle units, these values fell within the ranges expected for $E1$, $M1+E2$, and $E2$ transitions. Since the ground-state spin of Sc^{41} is $\frac{7}{2}^-$, these results eliminated from consideration assignments of $J^\pi=\frac{1}{2}^+$, $\frac{1}{2}^-$, and $\frac{3}{2}^+$ for the radiating states. For 16 of the most strongly excited levels, specific evidence with respect to possible values of J^π was obtained by measuring the angular distribution of the γ radiation emitted in transitions to the ground state. For ten additional states, earlier studies of proton elastic scattering furnished values of the orbital angular momentum l_p of the captured protons. These data permitted specific J^π assignments in 14 favorable cases, and restricted assignments to two values of J and either parity in ten cases. Eleven transitions are found to occur by means of either pure $E2$ or mixed $M1$ and $E2$ radiation. The combined strength of these transitions exhausts 6–8% of the $E2$ sum-rule limit. The present status of information on energies and values of J^π of the states of Sc^{41} occurring at excitation energies up to 6.2 MeV is summarized.

1. INTRODUCTION

THE level structure of the mirror nuclei Ca^{41} and Sc^{41} has been intensively investigated in the recent past by means of nucleon transfer reactions[1] and, in the case of Sc^{41}, by studies of proton elastic scattering.[2] A major feature of the level structure to emerge from this work is the abundance of levels, approximately 60 in the range of excitation energy up to 6 MeV. Few of these levels are found to have substantial single-particle widths; indeed, only three might really qualify in this respect. These results differ markedly from earlier expectations based on a simple shell-model description of these nuclei, in which only single-particle levels are predicted. The experimental evidence thus emphasizes the role of excited configurations of the Ca^{40} core in determining the level structure. Identification of these configurations then becomes a problem of considerable theoretical interest, requiring for its solution as much detailed spectroscopic data as possible. Among the additional pieces of experimental information that would be desirable are the spin assignments for the levels. Only a few assignments have been furnished by the earlier investigations, which characteristically determined l rather than J. The $Ca^{40}(p,\gamma)Sc^{41}$ reaction affords a convenient means for acquiring complementary data bearing on this question. Indeed, because of several special features of the (p,γ) reaction in this case, information of broader scope than usual can be obtained.

Because the Q value of the reaction[3] is but 1.08 MeV, it is energetically possible for all excited states to be directly populated by proton capture. Furthermore, the positron decay of the ground state of Sc^{41} [$E_{max}(\beta^+)=5.5$ MeV, $\tau_{1/2}=0.6$ sec] enables one to detect radiative capture events with great sensitivity and, hence, to locate weak resonances in the reaction cross section. This feature is of considerable practical value when taken together with the fact that all excited states of Sc^{41} are unstable to proton emission. Because of this, the occurrence of positron activity is strong evidence for capture transitions proceeding directly to the ground state. Such transitions will ordinarily be of the favored dipole and quadrupole types, and will occur from states whose values of J^π are compatible with these multipoles in transitions to the $\frac{7}{2}^-$ ground state. Thus, in the absence of cascade transitions, a measurement of the positron activity as a function of proton energy concentrates attention chiefly on those

* Work supported in part by the U. S. Atomic Energy Commission.

† Present address: The Cyclotron Institute, Texas A & M University, College Station, Tex.

‡ Present address: Oak Ridge National Laboratory, Oak Ridge, Tenn.

[1] Investigations of Ca^{41} by means of nucleon transfer reactions are reported by several groups including T. A. Belote, A. Sperduto, and W. W. Buechner, Phys. Rev. **139**, B80 (1965); R. Bock, H. H. Duhm, and R. Stock, Phys. Letters **18**, 61 (1965); K. K. Seth, R. G. Couch, J. A. Biggerstaff, and P. D. Miller, Phys. Rev. Letters **17**, 1294 (1966); T. A. Belote, Fu Tak Dao, W. E. Dorrenbusch, J. Kuperus, and J. Rapaport, Phys. Letters **23**, 480 (1966); and T. A. Belote, F. T. Dao, W. E. Dorrenbusch, J. Kuperus, J. Rapaport, and S. M. Smith, Nucl. Phys. **A102**, 462 (1967). Similar investigations of Sc^{41} are reported by H. E. Wegner and W. S. Hall, Phys. Rev. **119**, 1654 (1960); B. E. F. Macefield, J. H. Towle, and W. G. Gilboy, Proc. Phys. Soc. (London) **77**, 1050 (1961); G. F. Knoll, J. S. King, and W. C. Parkinson, Phys. Rev. **131**, 331 (1963); D. M. Sheppard, H. A. Enge, and H. Y. Chen, Bull. Am. Phys. Soc. **10**, 25 (1965); R. Bock, H. H. Duhm, and R. Stock, Phys. Letters **18**, 61 (1965).

[2] N. A. Brown and C. M. Class, Bull. Am. Phys. Soc. **8**, 127 (1963); N. A. Brown, Ph.D. thesis, Rice University, 1963 (unpublished).

[3] D. H. Youngblood, J. P. Aldridge, III, and C. M. Class, Nucl. Phys. **65**, 602 (1965).

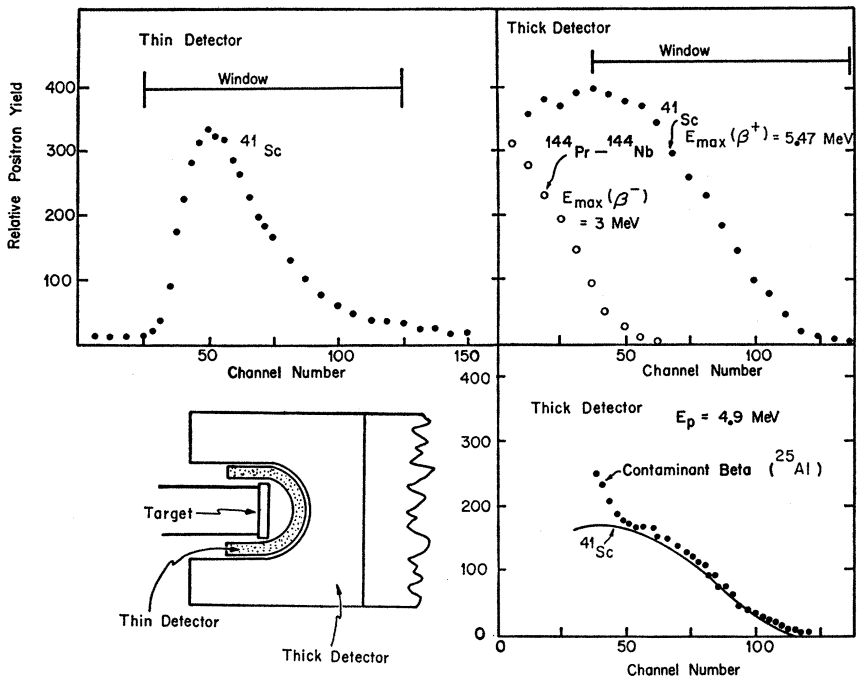

FIG. 1. In the lower left-hand panel, the standard arrangement of the thick and thin scintillation detectors with respect to each other and the target (source) is shown. In the two upper panels, coincidence-gated pulse-height spectra due to the Sc^{41} positron activity are plotted to show the characteristic response of each detector. The response to a lower-energy β activity is also included in the case of the thick detector. The plot in the lower right-hand panel is a spectrum obtained with the thick detector. It shows the deviation from the normal Sc^{41} spectral shape which occurred at some higher bombarding energies owing to the presence of a contaminant activity, believed to be Al^{25}.

states having spins of $\frac{5}{2}$, $\frac{7}{2}$, and $\frac{9}{2}$, and either parity. Such states, for which $l_p \geq 2$, may belong either to the group known previously from the elastic scattering measurements or to a new group of states whose proton widths were beneath the threshold for detection by such means. By broadening the scope of the (p,γ) measurements to include an absolute determination of the positron flux for each capture resonance, it is possible to obtain the radiative widths of the states—except for a statistical factor. With such results to supplement primary data drawn from measurements of γ-ray angular distributions and proton scattering, unambiguous spin-parity assignments to states can be made in favorable cases and, in others, the range of possibilities can be narrowed to several choices. By taking advantage of these circumstances in the work to be described below, it has been possible to make a substantial addition to the body of information available on Sc^{41}.

2. EXPERIMENTAL APPARATUS AND PROCEDURE FOR THE POSITRON MEASUREMENTS

The measurements described herein were carried out with the proton beam of the 5.5-MeV Van de Graaff accelerator of the Bonner Nuclear Laboratories. The beam was analyzed by magnetic deflection through 90° and was directed horizontally into the target chamber some 15 ft distant. The path and energy of the beam were defined by slits placed both at the entrance and exit of the magnet and at the entrance to the target chamber. Another set of slits situated between the magnet and chamber provided the signal for voltage stabilization of the accelerator. With proper adjustment of the slit widths, the spread in beam energy was reduced to 0.03% of the beam energy.

A. Energy Calibration of Accelerator

The energy of the protons was determined in terms of the resonance frequency of a nuclear-resonance magnetometer which had its probe located in the field of the 90° analyzing magnet. The frequency scale of the magnetometer was related to the proton energy scale on the basis of the frequencies measured at the thresholds of the $Li^7(p,n)Be^7$ and $C^{13}(p,n)N^{13}$ reactions. The threshold energies of these reactions were taken to be 1.8807 ± 0.0004 and 3.2358 ± 0.0011 MeV, respectively.[4] Repeated determinations of the threshold frequencies fell within a frequency interval corresponding to ±0.5 keV during periods in which slit settings were undisturbed. Using the calibration obtained from these measurements, we determined a value of 4.238 ± 0.004 MeV for the $F^{19}(p,n)Ne^{19}$ threshold. Within the combined errors, this agrees with the accepted value[4] of 4.233 ± 0.003 MeV.

The energies of five prominent $Ca^{40}(p,\gamma)Sc^{41}$ reaction resonances, spaced over the energy range investigated, were carefully determined immediately after calibration with the (p,n) thresholds. These served as secondary energy standards for various portions of the experimental program.

B. β-Detection Apparatus

The arrangement of the target and the detection apparatus is shown in Fig. 1. Targets were made by

[4] J. B. Marion, Rev. Mod. Phys. 33, 139 (1961); 33, 623 (1961).

evaporating natural calcium metal, assayed to be 99.5% pure,[5] onto gold foils 100 mg/cm² thick. The foils were in the normal target position as the terminal element of the beam tube assembly during evaporation. Such foils absorbed the proton beam but transmitted positrons with negligible energy losses. The target region was isolated from contaminants elsewhere in the vacuum system by encasing a section of beam tube 1 m long in a liquid-nitrogen bath.

The β radiation from the source was measured with a β-ray spectrometer of low resolving power consisting of two nested plastic scintillators arranged, as shown in Fig. 1, to subtend a large solid angle at the target. Positrons having an energy of about 5.5 MeV—corresponding to the end-point energy of the Sc^{41} spectrum—lost approximately 900 keV in traversing the thin inner detector and were completely absorbed by the thicker outer detector.

Each scintillator was optically coupled to a Dumont 6363 photomultiplier tube whose output, after amplification, was routed to a coincidence circuit operating with a resolving time of 60 nsec. Parallel outputs from the photomultipliers, after amplification and delay, were routed into two sections of a multichannel analyzer, each section being gated by the output signal from the coincidence unit. Thus, the pulse height from each detector could be recorded independently for each coincident event.

The excitation function of the $Ca^{40}(p,\gamma)Sc^{41}$ reaction was measured by counting the number of coincident events, for a specified accumulated charge, as a function of beam energy. The contribution of background to the counting rate during measurement of the Sc^{41} activity was much reduced by the coincidence requirement. It was reduced further by setting a discriminator on the amplified output of the thick scintillator so as to pass to the coincidence unit only those pulses corresponding to initial positron energies between 2.5 and 5.5 MeV. This restriction eliminated interference from a number of possible low-energy β activities arising from light elements present as contaminants in the target.

The pulse-height spectrum from the thick detector yielded a low-resolution energy spectrum of the detected β radiation. The pulse-height scale was calibrated in terms of energy with standard β sources and with the high-energy edges of Compton recoil electrons from γ-ray sources by use of procedures described by Cramer.[6] At each maximum in the excitation function, the energy spectrum from the thick detector was compared with a stored Sc^{41} spectrum to verify that the observed activity did in fact derive from Sc^{41}. Figure 1 shows the pulse-height spectra obtained from the two detectors, when operating in coincidence, with a Sc^{41} source. The discriminator windows used in measuring the excitation function are indicated. Also shown are the spectra obtained with the thick detector looking at a Ce^{144}-Pr^{144} source [$E_{max}(\beta^+)=2.98$ MeV][7] and at a Sc^{41} resonance at a higher bombarding energy where a contaminant β attributed to Al^{25} [$E_{max}(\beta^+)=3.25$ MeV][8] is observed superimposed on the Sc^{41} spectrum.

C. Beam Deflection

In order to enhance the detection sensitivity for the Sc^{41} activity with respect to prompt, beam-associated radiation, the detectors recorded events only when the proton beam was electrostatically deflected off the target and onto a gold beam catcher located 1 m upstream from the target chamber. The time 2τ for a complete deflection cycle was approximately 200 msec. In each cycle the detectors were turned on at $t_1 \approx 5$ msec after the beam was deflected off the target, and were turned off at $\tau - t_2 \approx 2$ msec before the beam was deflected back onto the target. The detectors were paralyzed during their "off" period by applying a negative voltage to the focusing electrodes of the photomultiplier tubes.

In order to evaluate the absolute β yield, one requires the relationship between the flux Y_{obs} (measured under the circumstances described) and the total number N of decaying Sc^{41} nuclei. On the assumption that the intensity of the proton beam is constant and that the bombardment has continued for $\sim$10 half-lives, this relationship is

$$N=\frac{\lambda\tau(1-e^{-2\lambda\tau})f(\Omega,E)Y_{obs}}{(1-e^{-\lambda\tau})(e^{-\lambda t_1}-e^{-\lambda t_2})},$$

where τ, t_1, and t_2 are as defined above, λ is the decay constant of the activity in question, and $f(\Omega,E)$ is the efficiency of the detector (a factor to be discussed in the following section).[9] The time intervals τ, t_1, and t_2 were measured to an uncertainty less than 1% by counting gated pulses from a 100-kc/sec crystal-controlled pulse source.

D. Detector Efficiency

The efficiency $f(\Omega,E)$ of the β-detection apparatus is a function both of the solid angle subtended and of the energy of the β radiation. The value of $f(\Omega,E)$ was obtained in a separate calibration measurement which utilized the β activity of F^{20} [$E_{max}(\beta^-)=5.40$ MeV, $\tau_{1/2}=11.4$ sec].[10] This activity has an end-point energy close to that of Sc^{41} and strong sources, free of contaminant activities of comparable half-life and end-

[5] Obtained from A. D. Mackay, Inc., 198 Broadway, New York, N. Y. 10038.

[6] J. G. Cramer, B. J. Farmer, and C. M. Class, Nucl. Instr. Methods **16**, 289 (1962).

[7] *Nuclear Data Sheets*, compiled by K. Way *et al.* (U. S. Government Printing Office, National Academy of Sciences–National Research Council, Washington, D. C.).

[8] P. M. Endt and C. Van der Leun, Nucl. Phys. **34**, 1 (1962).

[9] Corrections to take account of the customary small fluctuations of the beam intensity lead to negligible changes in the value of N.

[10] F. Ajzenberg-Selove and T. Lauritsen, Nucl. Phys. **11**, 1 (1959).

TABLE I. Data on levels observed in $Ca^{40}(p,\gamma)Sc^{41}$ reaction. The five energies identified by the symbol S are the energies of the prominent resonances used as secondary standards.

E_p (MeV)	E_{exc} (MeV)	Relative yield	$\int \sigma dE$ (eV b)	$g\Gamma_{\gamma g.s.}$ (eV)	Γ (keV)
0.648 ±0.002	1.714	0.021±0.001	0.017	0.0025	
1.540 ±0.003	2.584	0.070±0.002	0.035	0.013	
1.621 ±0.003	2.663	0.075±0.003	0.037	0.014	
S 1.8417±0.0015	2.879	1.0	0.450	0.193	
1.934 ±0.003	2.969	0.206±0.005	0.090	0.040	
2.153 ±0.003	3.182	0.644±0.019	0.262	0.131	
2.658 ±0.003	3.675	0.012±0.002	0.004	0.003	
S 2.6766±0.0020	3.692	1.276±0.016	0.448	0.279	
2.764 ±0.003	3.778	0.342±0.006	0.117	0.075	
3.010 ±0.003	4.018	0.280±0.007	0.092	0.064	
3.019 ±0.004	4.027	0.451±0.013	0.143	0.100	
3.240 ±0.004	4.242	0.666±0.009	0.205	0.154	
3.325 ±0.004	4.325	0.335±0.006	0.101	0.078	
3.440 ±0.004	4.437	0.212±0.006	0.062	0.050	
3.515 ±0.004	4.511	1.050±0.014	0.305	0.249	
S 3.8193±0.0030	4.808	1.155±0.014	0.316	0.280	
3.881 ±0.006	4.868	0.088±0.009	0.024	0.021	
3.965 ±0.005	4.950	1.120±0.030	0.287	0.265	2.4±0.6
S 4.0246±0.0030	5.008	2.053±0.041	0.541	0.506	
4.054 ±0.007	5.036	6.674±0.134	1.749	1.648	
4.160 ±0.009	5.140	0.04[a]	0.010	0.010	
S 4.1848±0.0045	5.164	3.354±0.167	0.859	0.836	
4.219 ±0.007	5.197	0.169±0.013	0.043	0.042	
4.244 ±0.009	5.222	0.08[a]	0.020	0.020	
4.346 ±0.007	5.321	0.407±0.025	0.101	0.102	
4.402 ±0.009	5.376	0.853±0.152	0.211	0.215	9.5±3.0
4.551 ±0.007	5.521	1.537±0.185	0.370	0.392	
4.564 ±0.009	5.534	0.26[a]	0.063	0.066	
4.596 ±0.009	5.565	0.48[a]	0.115	0.123	
4.602 ±0.010	5.571	0.33[a]	0.079	0.084	
4.683 ±0.007	5.650	0.95[a]	0.224	0.244	
4.724 ±0.010	5.690	0.16[a]	0.038	0.041	
4.741 ±0.010	5.706	3.66[a]	0.856	0.943	11.5±3.0
4.748 ±0.010	5.713	0.55[a]	0.129	0.142	
4.812 ±0.008	5.776	2.460±0.246	0.569	0.637	
4.835 ±0.008	5.798	0.34[a]	0.078	0.088	
4.850 ±0.008	5.813	0.944±0.300	0.217	0.245	
4.894 ±0.011	5.856	0.28[a]	0.064	0.073	
4.907 ±0.011	5.868	3.55[a]	0.810	0.923	9.4±2.0
4.952 ±0.011	5.912	0.40[a]	0.091	0.104	
5.011 ±0.011	5.970	1.05[a]	0.236	0.275	4.2±2.0
5.098 ±0.011	6.055	0.61[a]	0.135	0.160	3.9±1.0
5.127 ±0.011	6.083	0.15[a]	0.033	0.039	
5.154 ±0.011	6.109	0.84[a]	0.185	0.221	
5.158 ±0.011	6.113	1.81[a]	0.398	0.477	
5.191 ±0.011	6.145	2.16[a]	0.473	0.570	

[a] Within a factor of 2.

point energy, are easily produced by the $F^{19}(d,p)F^{20}$ reaction. The strength of the β activity available from resonances in the $Ca^{40}(p,\gamma)Sc^{41}$ reaction was insufficient for the Sc^{41} activity itself to be practical as the calibration source.

The steps involved in the calibration were as follows: To make a F^{20} source, F^{19} was evaporated onto a standard gold blank 100 mg/cm^2 thick, and was then bombarded with 2-MeV deuterons. The accompanying β activity was measured concurrently with a standard scintillation spectrometer of well-defined solid-angle and unit efficiency for all β energies of interest. Then a Fermi plot of the resulting energy spectrum was least-squares fitted by a straight line in the region above about 2.5 MeV where the data were linear. The equation of this line yielded the proportionality constant required to normalize the experimental spectrum to the theoretical spectrum for this allowed transition. The total flux of β's incident on the detector was then obtained by integrating the normalized theoretical spectrum. This procedure eliminated various small sources of uncertainty, such as γ-ray backgrounds, that distorted the shape of the lower-energy portion of the experimental spectrum. The good linearity and resolution of the energy response of the standard spectrometer were essential to the success of this procedure. The reliability of the fitting procedure was closely scrutinized and it was estimated that an uncertainty of 7% in the absolute flux of β's could be attributed to this source.

The F^{20} β spectrum was measured with the beam deflection technique described in the preceding section, and the formula given there was used to correct the "observed" flux of β's to the true total yield from the source, $f(\Omega,E)$ being in this case equal to the accurately known solid angle of the standard spectrometer. Thus, under the assumption of an isotropic distribution of β particles emanating from the source, the absolute yield of F^{20} β's per unit incident charge was estimated.[11]

The coincidence spectrometer was then placed at a convenient distance from the F^{20} source, with all operating parameters such as discriminator levels set as for the Sc^{41} measurements, and the coincidence yield was determined for a measured charge of deuterons delivered to the target. This established the efficiency $f(\Omega,E)$ of the coincidence spectrometer for a β spectrum characteristic of F^{20}. The thick-target flux of positrons from the strong $Ca^{40}(p,\gamma)Sc^{41}$ resonance at $E_p=1.842$ MeV was then measured, all parameters of the coincidence spectrometer remaining fixed.

The efficiency of the coincidence spectrometer for detection of the positrons from Sc^{41} was obtained from the value measured for F^{20} by making corrections to take account of various slight differences between the spectral shapes for F^{20} and Sc^{41}, including those differences caused by the presence of annihilation radiation in the latter case. The Sc^{41} efficiency thus obtained was used to convert the flux measured for the 1.842-MeV resonance into an absolute yield. After correction for the finite target thickness, the absolute thick-target yield obtained for this calibration resonance was $Y(\infty)=388\pm71$ positrons per μC of protons.

The uncertainty of 18% assigned to this result includes the aforementioned uncertainty of 7% arising from the fit to the Fermi plot and uncertainties of 2, 3, and 2.5% attributed, respectively, to counting statistics, calibration of the current integrator, and determination of the solid angle of the standard spectrometer. Additional contributions to the total uncertainty of 0.5 and 2% stem from the inexactness with which the window settings of the spectrometer and time

[11] The isotropy of the distribution of β's from the source on the gold backing foil was checked to within 10% at β energies greater than 3 MeV.

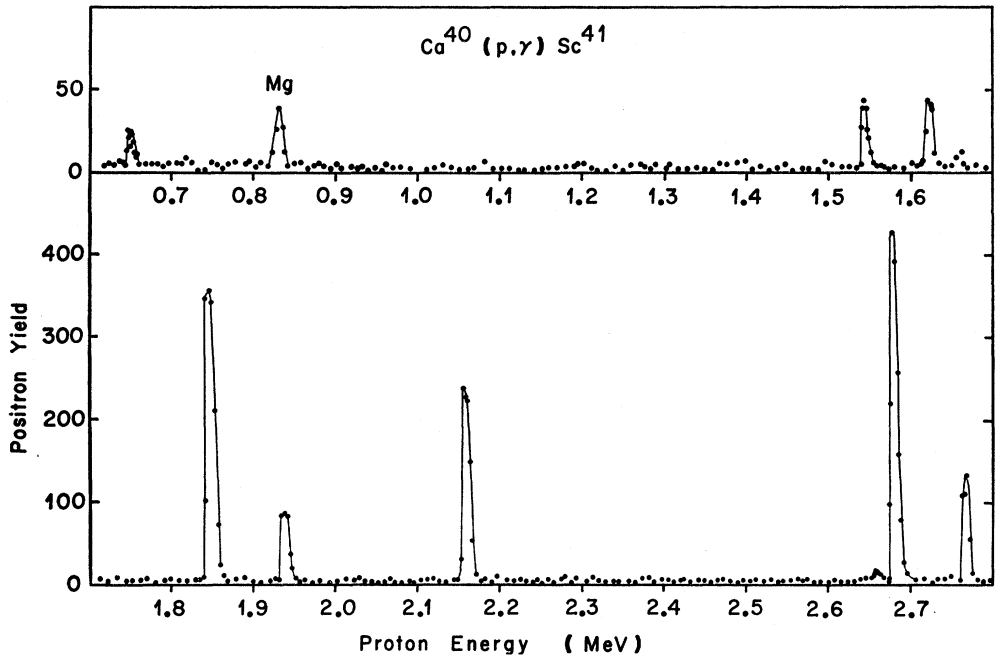

(a)

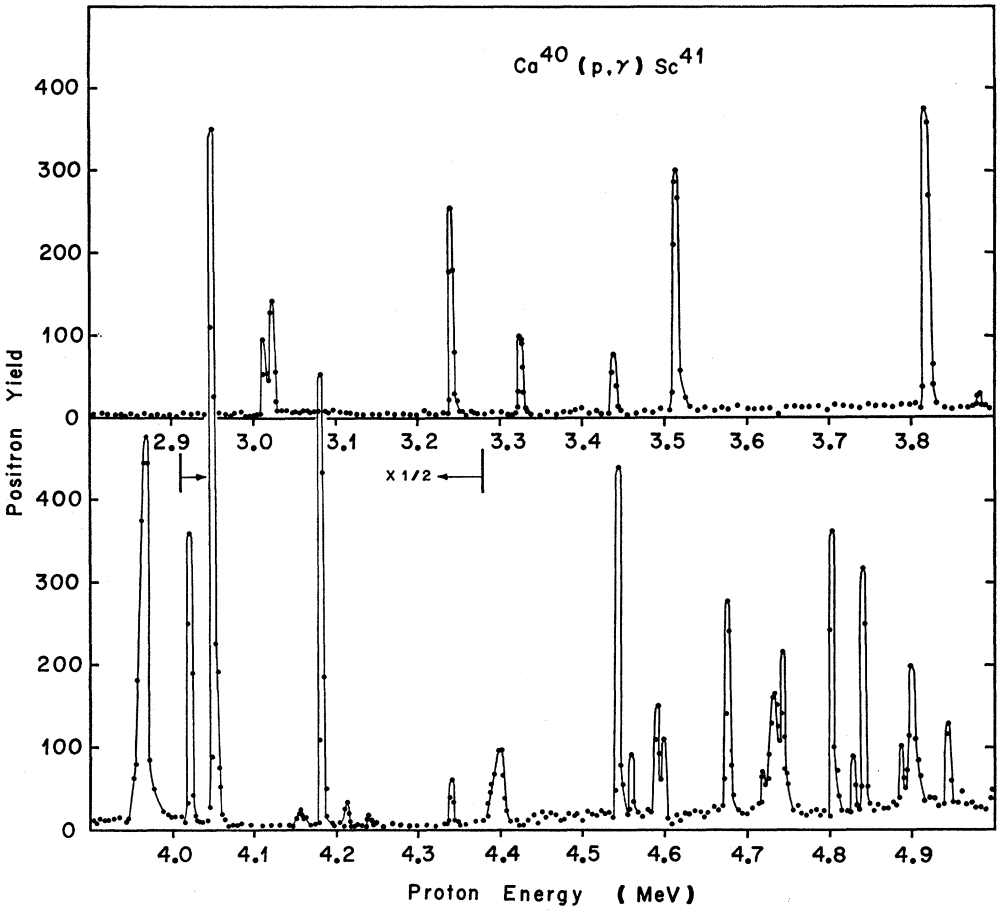

(b)

FIG. 2. The excitation function of the $Ca^{40}(p,\gamma)Sc^{41}$ reaction. No background has been subtracted.

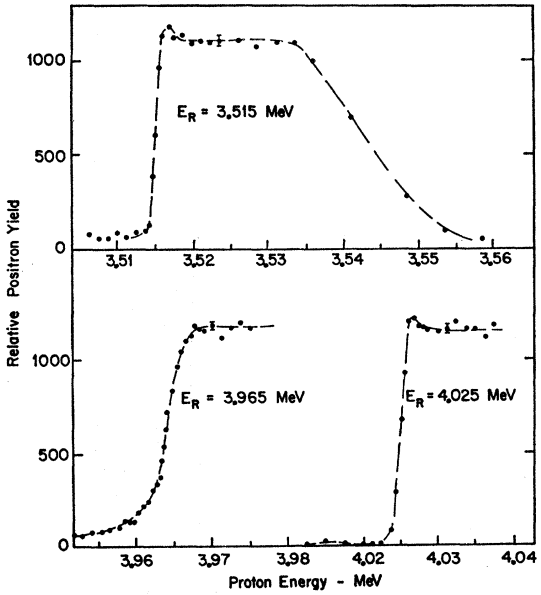

FIG. 3. Some selected thick-target yield curves. The interquartile distance of the lower-energy edge of the resonance step is about 1 keV for the resonances at 3.515 and 4.025 MeV, and 2.6 keV for that at 3.965 MeV.

constants of the beam deflection apparatus were known. A final contribution of 1% results from the uncertainty in the corrections that take into account the different response of the spectrometer to positrons and electrons.

3. RESULTS OF POSITRON MEASUREMENTS

The positron yield from "thin" calcium targets (2–10 keV thick for protons of appropriate energy) was measured as a function of proton energy from $E_{p(\mathrm{lab})} = 0.60$–$5.2$ MeV to provide the initial data. The resulting excitation function is presented in Fig. 2. The 46 resonances attributed to the $Ca^{40}(p,\gamma)Sc^{41}$ reaction on the basis of their spectra in the thick detector are listed in Table I.

Several weak maxima in the excitation function were attributed to the $Mg^{24}(p,\gamma)Al^{25}$ reaction, Mg being a known contaminant of the calcium target. This reaction yields positrons of 3.25-MeV end-point energy, and the energy spectra from the thick detector confirm that the maxima at $E_p = 0.83$ and 1.66 MeV arise from well-established resonances in this reaction.[8] At proton energies above 4.3 MeV, a gradually increasing continuum and a few very weak-intensity maxima (all corresponding to β activity of maximum energy between 2.8 and 3.4 MeV) were observed in addition to the Sc^{41} activity. This extraneous activity, which except at its peak contributed less than half of the off-resonance counting rate, was also attributed to Al^{25}. The remainder of the continuum yield proved after further investigation to be due to Sc^{41} activity produced by nonresonant capture processes.

The values for resonant energies, relative yields, and widths given in Table I were obtained from data taken with targets 20–30 keV thick for resonances below $E_p = 4.1$ MeV and 2–13 keV thick for resonances above that energy. The resonances for which data were obtained with the 2-keV target are identified in the Table by the superscript a. Thinner targets were necessary above 4.1 MeV because of both the increasing density of resonances and the increasing importance of the nonresonant yield proportional to the target thickness. The latter tended to obscure weak resonances when thicker targets were used.

The energy assigned to each resonance corresponds to the midpoint of the rise of the thick-target yield curve in each case in which such data were available. These values were not corrected for the Lewis effect and the noninfinite thickness of the targets because these were negligible in comparison with uncertainties from other sources.

As mentioned earlier, five prominent resonances served as secondary energy standards. These resonances are identified in the Table by the symbol S located adjacent to the appropriate energy values. The energies of these resonances were determined in terms of the primary calibration standards on three separate occasions; the stated values represent an average of these determinations. The uncertainties attached to these energies combine the uncertainties in the primary calibration energies with those involved in determining threshold and resonance frequencies from the data, and also include those caused by retuning the beam when repeating the measurements. The uncertainties assigned to the other resonances usually are larger for a variety of reasons—chiefly because of less sharp beam-tuning conditions and poorer statistics for resonances below 4.1 MeV, and greater uncertainty in picking resonance frequencies from the thin-target data for energies greater than 4.1 MeV. The excitation energy of each level in Sc^{41} is also listed, the values being calculated on the assumption that the Q value for the reaction is 1.082 MeV.[3,12]

The relative yields listed in Table I are those obtained after correction for the finite target thickness by use of the formula[13]

$$Y_{\max}(\xi)/Y_{\max}(\infty) = (2/\pi)\arctan(\xi/\Gamma'),$$

where Γ' is taken as the interquartile distance of the low-energy edge of the resonance step, $Y_{\max}(\xi)$ is the maximum yield measured for a target of thickness ξ, and $Y_{\max}(\infty)$ is the corrected yield corresponding to an infinitely thick target. For resonances below 4.1 MeV this correction amounted to only a few percent. The uncertainty attributed to the relative yield in these cases arises mainly from the statistical uncertainty in

[12] L. A. Konig, J. H. E. Mattauch, and A. H. Wapstra, Nucl. Phys. **31**, 18 (1962).
[13] W. A. Fowler, C. C. Lauritsen, and T. Lauritsen, Rev. Mod. Phys. **20**, 236 (1948).

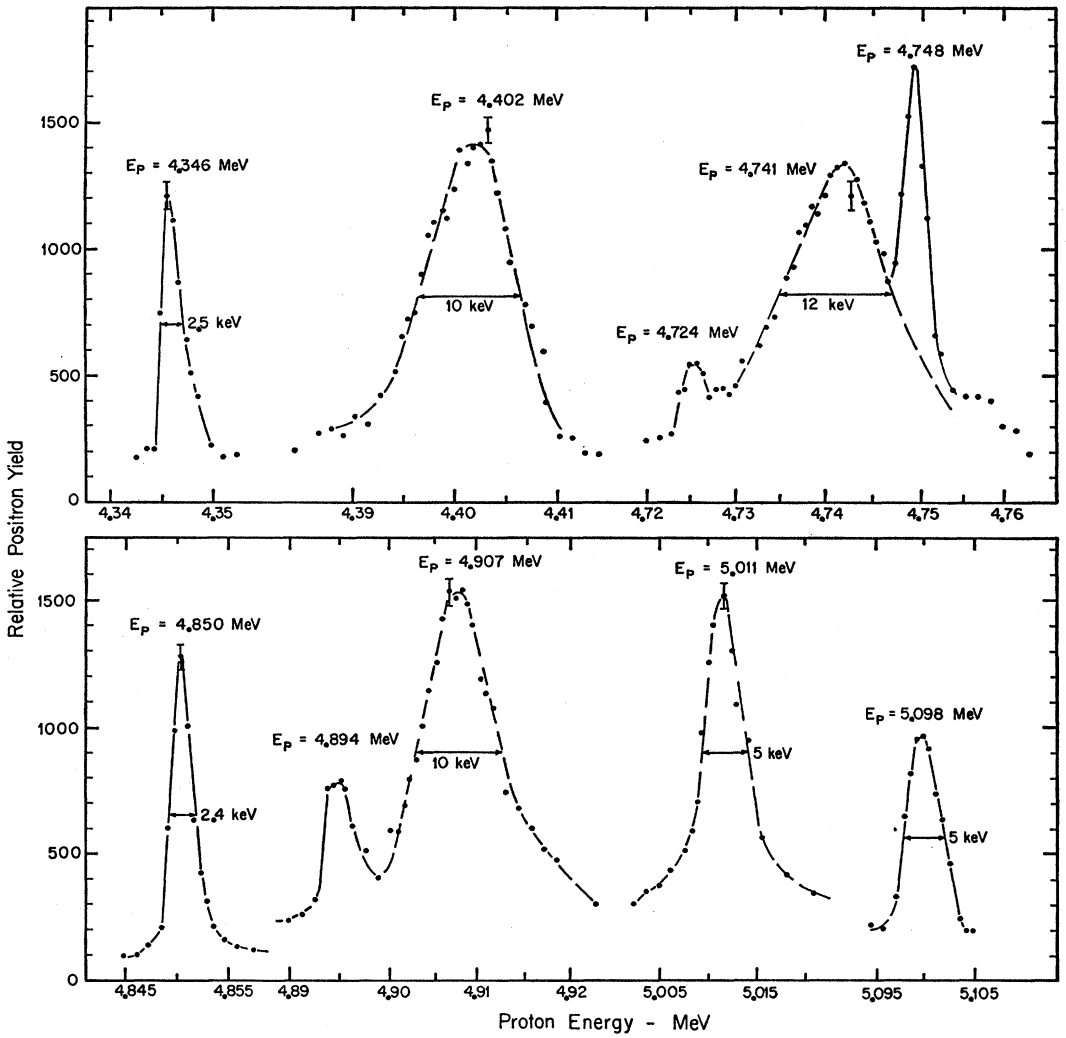

FIG. 4. Some selected thin-target yield curves for resonances showing widths either equal to or greater than the experimental resolution.

the definition of the plateau yields. For resonances above 4.1 MeV measured with thin targets, the corrections to the yields to take account of target thickness amounted to 30–40%. However, the corrected relative yields given in the Table could be uncertain to within an additional factor of 2 owing to inaccurate determinations of the actual magnitudes of the resonance maxima.

The thick-target yield curves in the vicinities of the 3.515-, 3.965-, and 4.025-MeV resonances are shown in Fig. 3. The value of the quantity Γ' is approximately 1 keV for the 3.515- and 4.025-MeV resonances, a value consistent with the dispersion δ in the beam energy. The width of the 3.965-MeV resonance is noticeably greater than this intrinsic experimental width, however, and its natural width Γ can be extracted by making use of the expression[13] $\Gamma'^2=\Gamma^2+\delta^2$. In measurements with a thin target, five other resonances above 4.1 MeV were observed to have widths greater than the experimental resolution width. The data for these cases are shown in Fig. 4. The natural widths for these levels were extracted by use of the expression

$$\Gamma''^2=\Gamma^2+\delta^2+\xi^2,$$

where Γ'' is the observed half-width of the resonance. It might be noted that the shapes of the resonances at E_p=4.402 and 4.741 MeV are rather unsymmetrical. This behavior could possibly result from unresolved weaker states. Their presence has not been considered in extracting the values of the widths. The total widths determined for these states are listed in Table I.

The integrated cross section for a resonance is obtained by using the formula $\int\sigma dE=(eAS/N)Y(\infty)$, where S is the stopping power of the target material, A is the atomic number of the target material, e is the charge of the proton, N is Avogardro's number, and

TABLE II. Comparison of previous and present results on the $Ca^{40}(p,\gamma)Sc^{41}$ reaction.

Resonance energy (MeV)		$\int\sigma dE$ (eV b)	
Previous[a]	Present	Previous[a]	Present
0.650±0.005	0.648±0.002	0.02	0.017±0.004
1.550±0.015	1.540±0.003	0.03	0.035±0.009
1.630±0.015	1.621±0.003	0.03	0.037±0.009
1.850±0.010	1.842±0.002	0.3	0.450±0.110
		0.30±0.05[b]	

[a] Reference 14. [b] Reference 15.

$Y(\infty)$ is the plateau yield from an infinitely thick target per unit incident charge. The value of $Y(\infty)$ is obtained by taking the product of the relative yield of the resonance, as listed in Table I, with the absolute yield of the $E_p=1.842$ MeV resonance, as determined during the calibration of the detectors. The values of $\int\sigma dE$ listed in Table I thus have uncertainties identical to those of the corresponding relative yields. Additional constant uncertainties in the integrated cross sections are contributed by the 18% uncertainty in the absolute yield of the 1.842-MeV resonance and the 7% uncertainty in the stopping power of calcium.

The intrinsic parameters of a state formed by proton capture are related to the integrated cross section for γ emission by the expression

$$2\pi^2 g\lambda\!\!\!^{-2}\Gamma_\gamma\Gamma_p/\Gamma=\int\sigma dE.$$

If it is assumed that $\Gamma_\gamma\ll\Gamma_p$, then the radiative width Γ_γ may be determined (apart from a statistical factor) by the expression

$$g\Gamma_\gamma=(2\pi^2\lambda\!\!\!^{-2})^{-1}\int\sigma dE,$$

where

$$g=(2J+1)/(2I+1)(2S+1).$$

Table I also lists the radiative widths thus extracted for the $Ca^{40}(p,\gamma)Sc^{41}$ resonances observed.

The data from which the integrated cross sections and the values of $g\Gamma_\gamma$ are obtained include only those capture events that result in the formation of Sc^{41} in its ground state. Because all of the excited states of Sc^{41} are unstable to proton emission, γ decay competes with generally faster particle emission. Hence a cascade transition to the ground state through an intermediate state is unlikely because it would involve a factor $(\Gamma_\gamma/\Gamma_p)^2\ll1$. Thus it is expected that the values of the integrated cross section and Γ_γ listed in Table I are primarily for direct ground-state transitions; this assumption is indicated by the subscript g.s. on the symbol Γ_γ. The γ-ray measurements, to be discussed in the following section, confirm that the direct decay predominates for those resonances studied by this means; and other evidence to be presented there also supports this conclusion.

Only one previous investigation of the $Ca^{40}(p,\gamma)Sc^{41}$ reaction has been reported[14]; the results pertinent to the present study are presented for comparison in Table II. The Table includes, in addition, an isolated result from the work of Engelbertink and Endt,[15] who studied the 1.842-MeV resonance as part of a program undertaken to measure the strengths of (p,γ) resonances in the *s-d* shell.

4. γ-RAY MEASUREMENTS

The γ rays emitted in transitions directly to the ground state of Sc^{41} at a number of capture resonances were sufficiently intense to make the study of their angular distributions practicable with conventional scintillation detectors. Sixteen cases were selected for investigation, all occurring at incident proton energies below 4 MeV, where the resonances are well spaced. The angular-distribution data obtained in this series of measurements provided the only information bearing directly on spin-parity assignments for 12 of the capture states involved. In the other cases, for which the angular momenta of the protons captured in forming the states were known from measurements of proton elastic scattering, the angular-distribution data gave a basis for a choice between the two possible values of J.

The detectors used for these measurements were two cylindrical NaI(Tl) crystals 12.7 cm in diameter and 12.7 cm long, each shielded by 5-cm-thick lead annuli and coupled to RCA 8055 photomultiplier tubes. The targets employed were prepared in an off-line evaporator by depositing layers of calcium metal to a thickness of 0.3 mg/cm^2 onto standard gold backings 300 mg/cm^2 thick. In order to inhibit oxygen contamination of the targets during transfer to the target chamber and during subsequent use, the calcium layer was coated with a film of gold 0.3–0.6 mg/cm^2 thick. Measurements by means of proton-elastic scattering showed that this procedure limited the oxygen contamination to less than 2% of the calcium present, even after the targets were used for extended periods of data collection. The beam currents to which these targets were subjected ranged from 2–8 μA. When the higher beam intensities were employed, 20-mil-thick tungsten blanks were substituted for the standard gold backings. The targets were cooled by forced air, and no loss of calcium from the target was observed when the beam currents were held within the stated limits.

In measuring the angular distributions, the target assembly was the same as described for the positron measurements except that the target plane was inclined at 45° with respect to the beam direction. The counter was mounted to rotate about a vertical axis through the target; the zero setting of the angular scale was accurate to within ±2° and the angular positions could

[14] J. W. Butler, Phys. Rev. **123**, 873 (1961).
[15] G. A. P. Engelbertink and P. M. Endt, Nucl. Phys. **88**, 12 (1966).

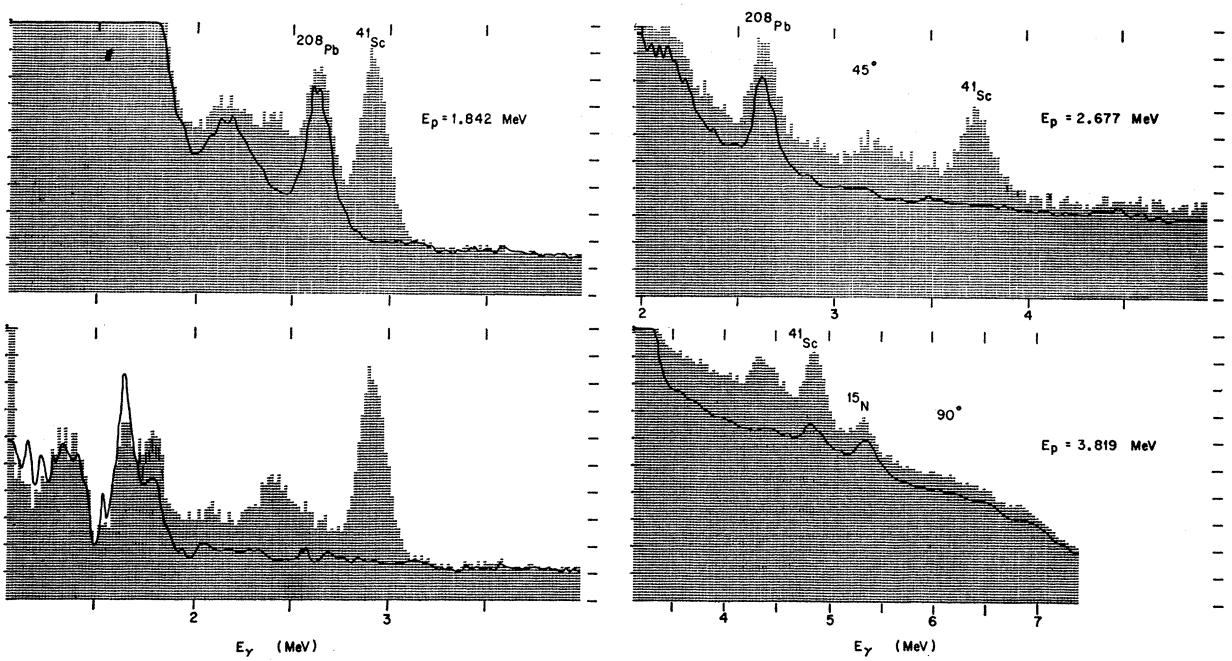

FIG. 5. Print-outs of γ-ray spectra. The vertical scales are linear.The spectra in the two left-hand panels were taken at the 1.842-MeV resonance. In the upper panel, both the on-resonance and off-resonance spectra are presented, the latter indicated by the line superimposed on the print-out. The lower panel shows the on-resonance spectrum after subtraction of room background. The superimposed spectrum is that taken off-resonance—after background subtraction. Note the absence of the 2.62-MeV peak due to Pb^{208} in these spectra. In the two right-hand panels are print-outs of spectra in the neighborhood of the full-energy γ-ray peaks, obtained at the 2.677- and 3.819-MeV resonances. The spectra indicated by the superimposed lines are those taken off-resonance in each case.

be reproduced to within 0.2°. The data were obtained in the forward quadrant containing the normal to the target plane. Differences in the attenuation of the γ-ray intensity in the thin target backings at the various angles of measurement were negligible for the γ rays of interest ($E_\gamma \geq 2$ MeV). The system, consisting of the target chamber and movable counter, was checked periodically for angular symmetry by measuring the angular distribution of the 3.09-MeV γ rays from the $C^{13}(p,p')C^{13}$ reaction, which is known to be isotropic. A second counter monitored the reaction and was usually positioned at an angle of 240°.

A selection of γ-ray spectra representative of those obtained in the angular-distribution measurements is shown in Fig. 5. As can be seen, the full-energy peaks of the γ rays emitted in transitions to the ground state of Sc^{41} are characteristically superimposed upon a strong continuous background. Investigation of this background showed it to arise chiefly from light-element impurities in the target material itself. In addition, the spectra include peaks due to γ rays from the residual room background, which are prominent at lower bombarding energies; and at higher bombarding energies there is evidence for the 5.3-MeV γ ray from the $O^{18}(p,\alpha)N^{15}$ reaction. The latter γ ray proved to be the most troublesome contaminant of the spectra, having an energy and intensity comparable to that of the Sc^{41} radiation at some resonances despite the aforementioned limit of 2% on the oxygen contamination of the target.

For the cases shown in Fig. 5, as well as all others investigated, no peaks attributable to Sc^{41} γ rays were discernible above background in the spectra, apart from those due to the direct transition to the ground state. The absence of detectable cascades in these measurements supports the assumption made in the preceding section that only transitions directly to the ground state contribute to the integrated positron yields.

5. ANGULAR DISTRIBUTIONS

γ-ray spectra were measured at each resonant energy of interest for 3–5 angular positions of the movable detector. Off-resonance spectra, necessary for background subtraction, were measured at bombarding energies roughly 50 keV below the resonant energies. For most cases, one off-resonance spectrum at a single angular setting of the movable detector was sufficient; but for resonances at which radiation from the competing $O^{18}(p,\alpha)N^{15}$ reaction was intense, more detailed background data were necessary. Concurrent with all the foregoing measurements, spectra were also taken with the fixed monitor detector.

Net normalized intensities of the Sc^{41} γ rays were obtained from these data by first subtracting room background from each spectrum, and then subtracting the off-resonance spectra from corresponding on-resonance spectra. In the subtraction process, an internormalization was used such that the resulting spectra

TABLE III. Coefficients a_2 and a_4 of the expansion $W(\theta)=1+a_2P_2(\cos\theta)+a_4P_4(\cos\theta)$ describing the fit to the angular-distribution data obtained at each resonance, $P_j(\cos\theta)$ being the Legendre polynomial of order j. The coefficients were determined by a least-squares fitting procedure, and have been corrected for the finite solid angle of the γ-ray detector.

E_p (MeV)	E_{exc} (MeV)	a_2	a_4
1.540	2.584	−1.02 ±0.09	0.117±0.171
1.621	2.663	−0.30 ±0.14	0.385±0.244
1.842	2.879	0.507±0.023	−0.025±0.031
1.934	2.969	0.722±0.079	−0.107±0.127
2.153	3.182	−0.395±0.017	0.017±0.026
2.677	3.692	0.536±0.033	−0.008±0.046
2.764	3.778	−0.138±0.050	−0.027±0.078
3.010	4.018	0.506±0.015	−0.332±0.022
3.019	4.027	0.450±0.035	−0.024±0.052
3.240	4.242	−0.217±0.039	0.055±0.056
3.440	4.437	0.483±0.233	0.411±0.344
3.515	4.511	−0.394±0.024	0.013±0.023
3.819	4.808	−0.408±0.023	0.031±0.032
3.965	4.950	−0.507±0.081	0.013±0.097
4.025	5.008	0.564±0.042	−0.165±0.054
4.054	5.036	−0.215±0.021	−0.069±0.025

had net null intensities for γ-ray energies greater than the maximum possible from the Sc^{41} decay. The rationality of this procedure was checked by comparing line shapes in the reduced spectra with the shapes of standard undistorted lines of comparable energy previously measured with the detector. The area corresponding to the full-energy peak, or to the full-energy plus single-escape peak, of the Sc^{41} γ-ray line then was taken as the unnormalized yield of the ground-state transition in each spectrum. Finally, these yields were normalized from angle to angle by use of the corresponding yields from the monitor detector.

The statistical probable errors in the final normalized intensities range from 1 to 10%. An additional uncertainty arising from background subtraction amounts to from 3 to 20%, depending upon the resonance. These magnitudes were estimated by studying the dependence of net yield upon the region of γ-ray energy used to normalize the off-resonance spectra to the on-resonance data. Finally, in the case of four resonances at which the capture radiation was imperfectly resolved from radiation due to the $O^{18}(p,\alpha)N^{15}$ reaction, the specific method of subtraction introduced some further uncertainty in the yields. This was estimated to range from 5 to 15% for the various examples.

The information gathered about the ground-state transition for each of the 16 Sc^{41} levels investigated was thus reduced to a set of intensities at 3–5 angles of emission relative to the direction of the incident beam, and the estimated errors of each of these intensity values. These results are summarized in Table III. Each set of experimental data was then analyzed in terms of the well established theory of the angular distribution of γ radiation emitted from sharp resonant states.[16] Theoretical angular distributions of the radiation emitted from levels of spins $\frac{3}{2}$, $\frac{5}{2}$, $\frac{7}{2}$, and $\frac{9}{2}$ to a level of spin $\frac{7}{2}$ (the ground-state spin of Sc^{41}) were calculated for values of the mixing parameter δ (the ratio of the amplitude of the higher-order multipole radiation to that of the lower-order amplitude) which ranged from $\arctan\delta=+90°$ to $-90°$ in 2° intervals. Every experimental angular distribution was compared in turn with each calculated distribution, and the quality of the fit was expressed in terms of the quantity

$$\chi^2=\sum_{i=1}^{N}\left[\frac{\sigma_i(\text{expt})-\sigma_i(\text{calc})}{\Delta\sigma_i(\text{expt})}\right]^2,$$

where N is the number of experimental points or angles. The results of this analysis, for each of the levels studied, are presented in the panels of Fig. 6, with the values of $\chi^2/(N-n)$ plotted against the values of $\arctan\delta$ for each of the assumed spins of the resonance levels. Here $(N-n)$ is the number of degrees of freedom used in the fitting procedure. The horizontal lines in each case in Fig. 6 indicate the limits which the value of $\chi^2/(N-n)$ would exceed with only a 1% probability for a legitimate fit to the data.[17]

From examination of Fig. 6 it can be seen that in most instances the theoretical angular distributions for two or more values of spin of the capture state are consistent with the experimental data. This multiplicity of possible spin values of a level is a normal situation when only a single angular distribution is analyzed, and additional physical information is usually needed in order to specify the spin. The absence of detectable branch decays of the levels of Sc^{41} removes a valuable source of this additional information. However, the information about the radiative widths of the levels (which is available from the positron work) and the knowldege of the l_p values of some of the states [which is available from a study of the $Ca^{40}(p,p)Ca^{40}$ reaction[2]] does provide a basis for establishing unique values in a number of cases, as will now be discussed.

6. DISCUSSION OF SPIN-PARITY ASSIGNMENTS

All data bearing on spin-parity assignments for states observed in the $Ca^{40}(p,\gamma)Sc^{41}$ experiment are summarized in Tables IV and V. Table IV contains results for 14 states observed both in the (p,p) experiment and in the present study. States excited by these reactions were assumed to correspond if their energies differed by less than the combined errors of the measurements. Actually, no energy difference exceeds 5 keV for the states considered. For four of these 14 states, there is complete

[16] W. J. Sharp, J. M. Kennedy, B. J. Sears, and M. G. Hoyle, Atomic Energy Commission of Canada Report No. 97, CRT-556, 1953 (unpublished).

[17] A. H. Wapstra, G. J. Nijgh, and R. van Lieshout, *Nuclear Spectroscopy Tables* (North-Holland Publishing Co., Amsterdam, 1959), p. 16.

TABLE IV. Summary of data on Sc^{41} levels derived from the present (p,γ) measurements and earlier studies of proton elastic scattering.

Excitation energy (p,γ) (MeV)	Excitation energy (p,p)[a] (MeV)	l_p[a]	J_i^π (possible)[b]	Γ_γ (eV)	δ[c]	$\lvert M(L)\rvert^2$[d] (W.u.)		$\lvert M(L+1)\rvert^2$[d] (W.u.)		J_i^π (preferred)
3.778	3.779	2	$\frac{3}{2}^+$	3.8×10^{-2}	$0.29_{-0.17}^{+0.17}$	2.6×10^{2}	$M2$	6.9×10^{3}	$E3$	$\frac{5}{2}^+$
			$\frac{5}{2}^+$	2.5×10^{-2}	0 ± 0.11	5.7×10^{-4}	$E1$	0	$M2$	
4.242	4.244	2	$\frac{3}{2}^+$	7.7×10^{-2}	$0.33_{-0.16}^{+0.14}$	2.8×10^{2}	$M2$	7.9×10^{3}	$E3$	$\frac{5}{2}^+$
			$\frac{5}{2}^+$	5.1×10^{-2}	$0.035_{-0.035}^{+0.11}$	8.2×10^{-4}	$E1$	0.25	$M2$	
4.868	4.864	2	$\frac{3}{2}^+$	1.05×10^{-2}	···	22	$M2$	4.2×10^{3}	$E3$	$\frac{5}{2}^+$
			$\frac{5}{2}^+$	7×10^{-3}	···	7.5×10^{-5}	$E1$	14	$M2$	
4.950	4.947	3	$\frac{5}{2}^-$	8.8×10^{-2}	$0.25_{-0.09}^{+0.09}$	3.26×10^{-2}	$M1$	0.25	$E2$	$\frac{5}{2}^-$
5.036	5.031	4	$\frac{7}{2}^+$	4.1×10^{-1}	$0.70_{-0.45}^{+0.78}$	2.7×10^{-3}	$E1$	2.3×10^{2}	$M2$	$\frac{9}{2}^+$
			$\frac{9}{2}^+$	3.3×10^{-1}	$0.035_{-0.035}^{+0.26}$	3.2×10^{-3}	$E1$	0.7	$M2$	
5.140	5.139	1	$\frac{1}{2}^-$	1.0×10^{-2}	···	1.1×10^{5}	$M3$	2.9×10^{7}	$E4$	$\frac{3}{2}^-$
			$\frac{3}{2}^-$	5×10^{-3}	···	0.2	$E2$	5.5×10^{4}	$M3$	
5.376	5.371	2	$\frac{3}{2}^+$	10.8×10^{-2}	···	135	$M2$	2.2×10^{4}	$E3$	$\frac{5}{2}^+$
			$\frac{5}{2}^+$	7.2×10^{-2}	···	5.7×10^{-4}	$E1$	90	$M2$	
5.571	5.571	2	$\frac{3}{2}^+$	4.2×10^{-2}	···	44	$M2$	6.5×10^{3}	$E3$	$\frac{5}{2}^+$
			$\frac{5}{2}^+$	2.8×10^{-2}	···	2.0×10^{-4}	$E1$	29	$M2$	
5.650	5.648	3	$\frac{5}{2}^-$	8.1×10^{-2}	···	2.1×10^{-2}	$M1$	2.0	$E2$	$\frac{5}{2}^-,\frac{7}{2}^-$
			$\frac{7}{2}^-$	6.1×10^{-2}	···	1.6×10^{-2}	$M1$	1.5	$E2$	
5.706	5.703	3	$\frac{5}{2}^-$	31.4×10^{-2}	···	8.0×10^{-2}	$M1$	7.5	$E2$	$\frac{5}{2}^-,\frac{7}{2}^-$
			$\frac{7}{2}^-$	23.6×10^{-2}	···	6.0×10^{-2}	$M1$	5.6	$E2$	
5.856	5.857	1	$\frac{1}{2}^-$	7.3×10^{-2}	···	3.2×10^{5}	$M3$	6.6×10^{7}	$E4$	$\frac{3}{2}^-$
			$\frac{3}{2}^-$	3.6×10^{-2}	···	0.75	$E2$	1.6×10^{5}	$M3$	
5.868	5.866	3	$\frac{5}{2}^-$	30.8×10^{-2}	···	7.3×10^{-2}	$M1$	6.4	$E2$	$\frac{5}{2}^-,\frac{7}{2}^-$
			$\frac{7}{2}^-$	23.1×10^{-2}	···	5.4×10^{-2}	$M1$	4.8	$E2$	
5.970	5.967	3	$\frac{5}{2}^-$	9.2×10^{-2}	···	2.1×10^{-2}	$M1$	1.75	$E2$	$\frac{5}{2}^-,\frac{7}{2}^-$
			$\frac{7}{2}^-$	6.9×10^{-2}	···	1.5×10^{-2}	$M1$	1.3	$E2$	
6.145	6.141	2	$\frac{3}{2}^+$	28.5×10^{-2}	···	182	$M2$	2.2×10^{4}	$E3$	$\frac{5}{2}^+$
			$\frac{5}{2}^+$	19×10^{-2}	···	1.0×10^{-3}	$E1$	122	$M2$	

[a] Reference 2.
[b] The possible values of J_i are given by $J_i=l_p\pm\frac{1}{2}$.
[c] The main value of δ is that corresponding to the minimum of χ^2 in each case. The upper and lower limits on δ are the values at which the χ^2-versus-$\tan^{-1}\delta$ curves cross the 1% probability lines.
[d] Transition strengths, expressed in Weisskopf units, for the lower and higher of the favored multipoles. The strengths were computed with the value of the mixing parameter δ determined by the minimum of the appropriate χ^2-versus-$\tan^{-1}\delta$ curve. Whenever no value of δ was known, the transition strengths were evaluated on the assumption that the transition was purely one or the other of the favored multipoles.

information (γ-ray angular distributions and values of $g\Gamma_\gamma$ and of l_p) upon which to base spin-parity assignments. For the remainder, only values of $g\Gamma_\gamma$ and l_p are known. Table V presents results for 12 states observed only in measurements of the (p,γ) reaction. The basic data in these cases consist of the γ-ray angular distributions and the values of $g\Gamma_\gamma$.

Considering first the contents of Table IV, the values of l_p entered for each state serve to limit the initial values of J_i^π to two possibilities corresponding to $l_p\pm\frac{1}{2}$. Only these values have been listed in the column labeled J_i^π (possible), notwithstanding the fact that in four cases γ-ray angular-distribution data suggested additional possibilities. The values of δ entered in the table for these cases correspond to the minima of the appropriate χ^2 curves of Fig. 6. The upper and lower bounds on these values are determined by the 1.0% criterion placed on the χ^2 test of the fit calculated for the tabulated values of J_i^π. The next column lists the values of Γ_γ obtained from the values of $g\Gamma_\gamma$ entered in Table I, after evaluation of the statistical factor g for the appropriate spin value J_i. The column headings $\lvert M(L)\rvert^2$ and $\lvert M(L+1)\rvert^2$ refer to the transition strengths, expressed in Weisskopf units, for the lower and higher of the favored multipoles, respectively. In cases in which no value of the mixing parameter δ is known, the transition strengths are evaluated on the assumption that the transition is purely one or the other of the favored multipoles.

The magnitudes of the transition strengths lead to unambiguous choices for the preferred values of J_i^π for states for which $l_p=1$ or 2, and these choices, either $\frac{3}{2}^-$ or $\frac{5}{2}^+$, are entered under the column heading J_i^π (preferred). The alternative choices of $J_i^\pi=\frac{1}{2}^-$ or $\frac{3}{2}^+$, respectively, lead to transition strengths far exceeding the empirically established maxima for these quantities. On the other hand, no such discrimination between the values of J_i^π is possible for the five $l_p=3$ states, since,

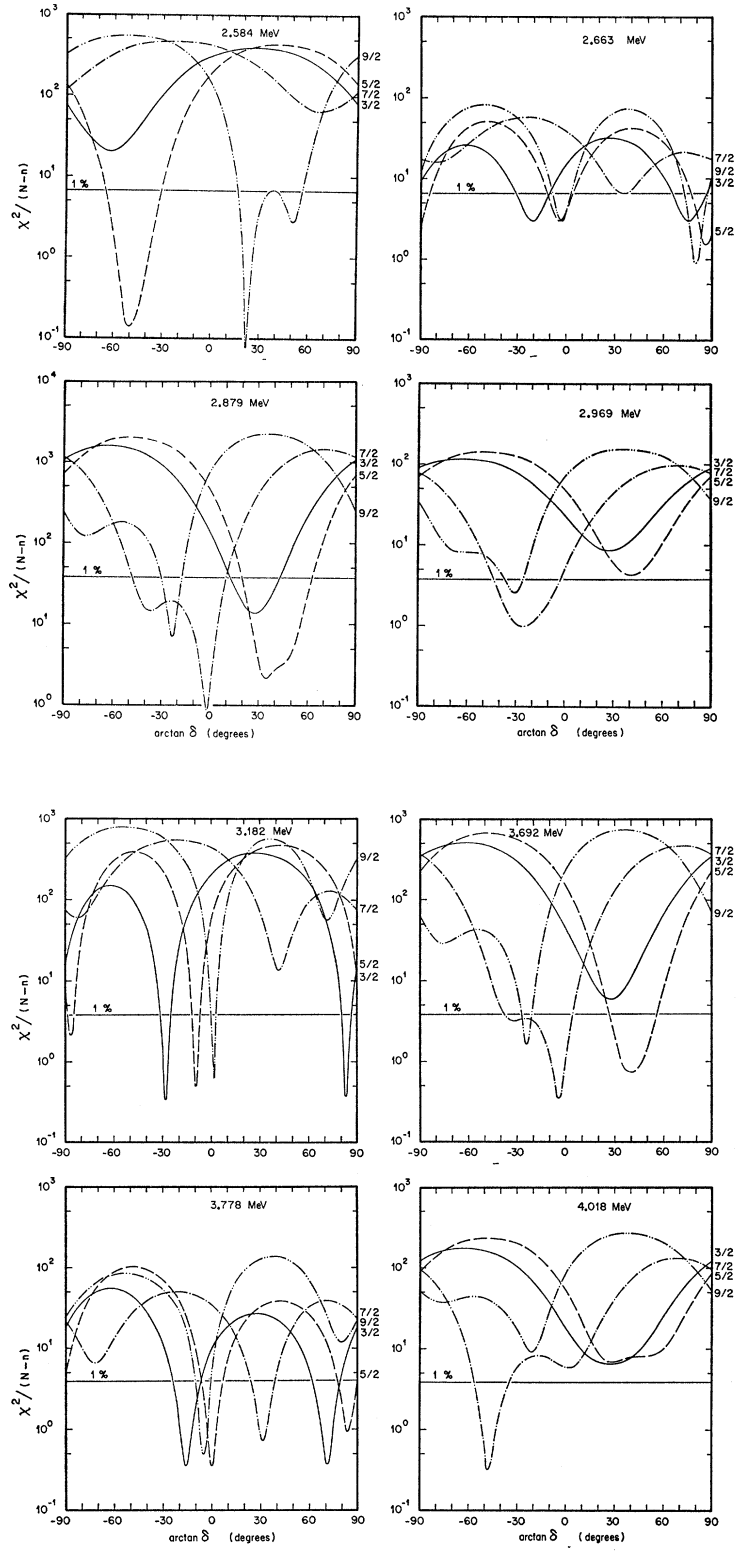

FIG. 6. Plot of χ^2 versus $\tan^{-1}\delta$ for the theoretical angular distributions of γ rays emitted from the various levels in transitions to the ground state, for possible values of J_i^π. Each horizontal line indicates the value of $\chi^2/(N-n)$ that would be exceeded with a probability of only 1% in the event of a legitimate fit to the data.

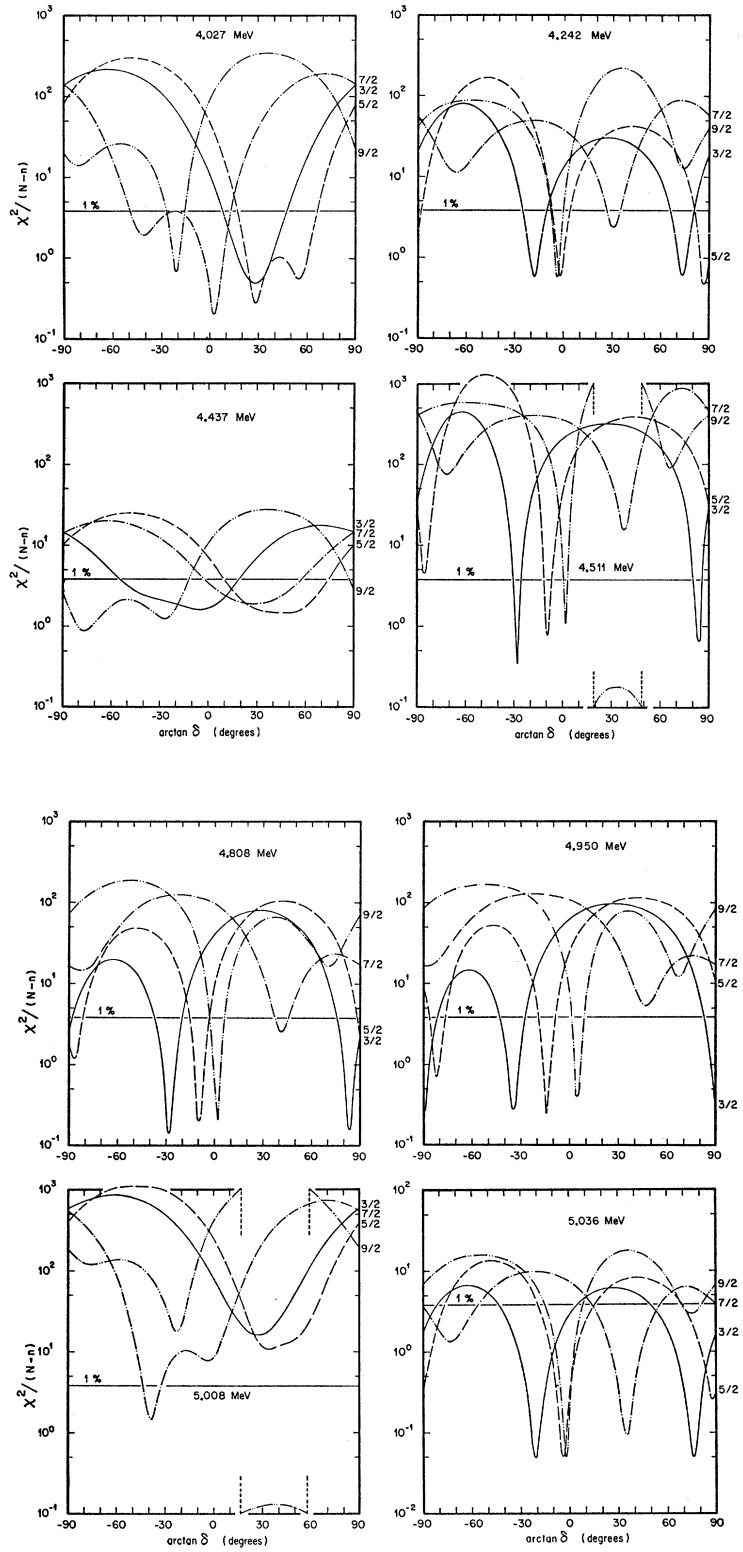

FIG. 6. (*Continued*).

TABLE V. Summary of data on Sc^{41} levels derived from the (p,γ) measurements.

E_{exc} (MeV)	J_i^π (possible)[a]	Γ_γ (eV)	δ[b]	$\lvert M(L)\rvert^2$[c] (W.u.)		$\lvert M(L+1)\rvert^2$[c] (W.u.)		J_i^π (preferred)
2.584	$\frac{5}{2}^+$	4.3×10^{-3}	$1.19_{-0.59}^{+1.05}$	1.3×10^{-4}	$E1$	1.3×10^{2}	$M2$	$\frac{5}{2}^-$
	$\frac{5}{2}^-$			5.0×10^{-3}	$M1$	3.4	$E2$	
	$\frac{9}{2}^+$	2.6×10^{-3}	$0.40_{-0.11}^{+1.08}$	1.6×10^{-4}	$E1$	19	$M2$	
2.663	$\frac{3}{2}^+$	7.0×10^{-3}	$0.36_{-0.18}^{+0.24}$	259	$M2$	2.2×10^{4}	$E3$	$\frac{5}{2}^\pm,\frac{9}{2}^+$
	$\frac{3}{2}^-$			6.7	$E2$	8.8×10^{5}	$M3$	
	$\frac{5}{2}^+$	4.7×10^{-3}	$0.07_{-0.07}^{+0.14}$	3.1×10^{-4}	$E1$	0.96	$M2$	
	$\frac{5}{2}^-$			1.2×10^{-2}	$M1$	2.5×10^{-2}	$E2$	
	$\frac{9}{2}^+$	2.8×10^{-3}	$0.035_{-0.035}^{+0.110}$	1.8×10^{-4}	$E1$	0.14	$M2$	
2.879	$\frac{5}{2}^+$	6.4×10^{-2}	$0.70_{-0.12}^{+0.45}$	2.2×10^{-3}	$E1$	6.0×10^{2}	$M2$	$\frac{7}{2}^-,(\frac{7}{2}^+,\frac{5}{2}^-)$
	$\frac{5}{2}^-$			8.6×10^{-2}	$M1$	15	$E2$	
	$\frac{7}{2}^+$	4.8×10^{-2}	$0.035_{-0.035}^{+0.12}$	2.5×10^{-3}	$E1$	1.7	$M2$	
	$\frac{7}{2}^-$			9.6×10^{-2}	$M1$	4.3×10^{-2}	$E2$	
2.969	$\frac{7}{2}^+$	1.0×10^{-2}	$0.47_{-0.42}^{+0.49}$	3.9×10^{-4}	$E1$	44	$M2$	$\frac{7}{2}^-,(\frac{7}{2}^+)$
	$\frac{7}{2}^-$			1.5×10^{-2}	$M1$	1.1	$E2$	
	$\frac{9}{2}^+$	8.0×10^{-3}	$0.58_{-0.09}^{+0.17}$	2.8×10^{-4}	$E1$	48.9	$M2$	
3.182	$\frac{3}{2}^+$	6.6×10^{-2}	$0.53_{-0.07}^{+0.09}$	886	$M2$	1.1×10^{5}	$E3$	$\frac{5}{2}^-,\frac{9}{2}^+$
	$\frac{3}{2}^-$			22.8	$E2$	4.6×10^{6}	$M3$	
	$\frac{5}{2}^+$	4.4×10^{-2}	$0.18_{-0.05}^{+0.04}$	1.6×10^{-2}	$E1$	24	$M2$	
	$\frac{5}{2}^-$			6.3×10^{-2}	$M1$	0.61	$E2$	
	$\frac{9}{2}^+$	2.6×10^{-2}	$0.035_{-0.035}^{+0.017}$	1.0×10^{-3}	$E1$	0.55	$M2$	
3.692	$\frac{5}{2}^+$	9.3×10^{-2}	$0.84_{-0.33}^{+0.64}$	1.3×10^{-3}	$E1$	3.1×10^{2}	$M2$	$\frac{5}{2}^-,\frac{7}{2}^\pm$
	$\frac{5}{2}^-$			5.2×10^{-2}	$M1$	8.1	$E2$	
	$\frac{7}{2}^+$	7.0×10^{-2}	$0.07_{-0.07}^{+0.71}$	1.7×10^{-3}	$E1$	2.8	$M2$	
	$\frac{7}{2}^-$			6.6×10^{-2}	$M1$	7.2×10^{-2}	$E2$	
	$\frac{9}{2}^+$	5.6×10^{-2}	$0.44_{-0.06}^{+0.09}$	1.20×10^{-3}	$E1$	24	$M2$	
4.018	$\frac{7}{2}^+$	1.6×10^{-2}	$1.11_{-0.41}^{+0.37}$	1.37×10^{-4}	$E1$	47	$M2$	$\frac{7}{2}^-$
	$\frac{7}{2}^-$			5.26×10^{-3}	$M1$	1.2	$E2$	
4.027	$\frac{3}{2}^+$	5.0×10^{-2}	$0.53_{-0.39}^{+0.57}$	207	$M2$	1.7×10^{4}	$E3$	$\frac{5}{2}^-,\frac{7}{2}^\pm$
	$\frac{3}{2}^-$			5.3	$E2$	6.6×10^{5}	$M3$	
	$\frac{5}{2}^+$	3.3×10^{-2}	$0.53_{-0.22}^{+1.73}$	4.9×10^{-4}	$E1$	38	$M2$	
	$\frac{5}{2}^-$			1.9×10^{-2}	$M1$	0.99	$E2$	
	$\frac{7}{2}^+$	2.5×10^{-2}	$0.05_{-0.05}^{+1.20}$	4.7×10^{-4}	$E1$	0.32	$M2$	
	$\frac{7}{2}^-$			1.8×10^{-2}	$M1$	8.5×10^{-3}	$E2$	
	$\frac{9}{2}^+$	2.0×10^{-2}	$0.38_{-0.09}^{+0.13}$	3.3×10^{-4}	$E1$	13	$M2$	
4.437	$\frac{3}{2}^+$	2.5×10^{-2}	$0.07_{-0.07}^{+1.60}$	81	$M2$	93	$E3$	$\frac{3}{2}^-,\frac{5}{2}^-,\frac{7}{2}^-$
	$\frac{3}{2}^-$			2.1	$E2$	3.7×10^{3}	$M3$	$(\frac{5}{2}^+,\frac{7}{2}^+)$
	$\frac{5}{2}^+$	1.7×10^{-2}	$1.04_{-0.87}^{+2.46}$	1.2×10^{-4}	$E1$	29	$M2$	
	$\frac{5}{2}^-$			4.5×10^{-3}	$M1$	0.7	$E2$	
	$\frac{7}{2}^+$	1.25×10^{-2}	$0.49_{-0.49}^{+1.11}$	1.4×10^{-4}	$E1$	7.9	$M2$	
	$\frac{7}{2}^-$			5.5×10^{-3}	$M1$	0.2	$E2$	
	$\frac{9}{2}^+$	1.0×10^{-2}	$0.49_{-0.28}^{+\infty}$	1.1×10^{-4}	$E1$	6.3	$M2$	
4.511	$\frac{3}{2}^+$	1.25×10^{-1}	$0.53_{-0.07}^{+0.07}$	293	$M2$	1.9×10^{4}	$E3$	$\frac{5}{2}^-,\frac{9}{2}^+$
	$\frac{3}{2}^-$			7.5	$E2$	7.5×10^{5}	$M3$	
	$\frac{5}{2}^+$	8.3×10^{-2}	$0.16_{-0.04}^{+0.05}$	1.09×10^{-3}	$E1$	6.2	$M2$	
	$\frac{5}{2}^-$			4.2×10^{-2}	$M1$	0.16	$E2$	
	$\frac{9}{2}^+$	5.0×10^{-2}	$0.035_{-0.035}^{+0.018}$	6.7×10^{-4}	$E1$	0.18	$M2$	
4.808	$\frac{3}{2}^+$	1.40×10^{-1}	$0.53_{-0.18}^{+0.25}$	239	$M2$	1.3×10^{4}	$E3$	$\frac{5}{2}^-,\frac{9}{2}^+,(\frac{7}{2}^-)$
	$\frac{3}{2}^-$			6.1	$E2$	5.4×10^{5}	$M3$	
	$\frac{5}{2}^+$	9.3×10^{-2}	$0.17_{-0.12}^{+0.12}$	1.0×10^{-3}	$E1$	5.7	$M2$	
	$\frac{5}{2}^-$			3.9×10^{-2}	$M1$	0.15	$E2$	
	$\frac{7}{2}^+$	7.0×10^{-2}	$0.86_{-0.19}^{+0.19}$	4.5×10^{-4}	$E1$	65	$M2$	
	$\frac{7}{2}^-$			1.7×10^{-2}	$M1$	1.7	$E2$	
	$\frac{9}{2}^+$	5.6×10^{-2}	$0.035_{-0.035}^{+0.09}$	6.2×10^{-4}	$E1$	0.15	$M2$	
5.008	$\frac{7}{2}^+$	1.3×10^{-1}	$0.81_{-0.16}^{+0.15}$	7.7×10^{-4}	$E1$	92	$M2$	$\frac{7}{2}^-$
	$\frac{7}{2}^-$			3.0×10^{-2}	$M1$	2.4	$E2$	

[a] The listed values of J_i^π(possible) are those whose value of χ^2 puts them within the 1% probability limit.

[b] The main value of δ is that corresponding to the minimum of χ^2 in each case. The upper and lower limits on δ are the values at which the χ^2-versus-$\tan^{-1}\delta$ curves cross the 1% probability lines. Only those roots of δ relevant to discrimination among spins have been entered in this column.

[c] Transition strengths, expressed in Weisskopf units (W.u.), for the lower and higher of the favored multipoles. The strengths were computed with the value of the mixing parameter δ determined by the minimum of the appropriate χ^2-versus-$\tan^{-1}\delta$ curve. Whenever no value of δ was known, the transition strengths were evaluated on the assumption that the transition was purely one or the other of the favored multipoles.

in all instances, the transition strengths for the $E2$ and $M1$ components for either of the possible spin choices fall within the presently established ranges for these quantities.

The foregoing description of the various headings in Table IV applies, with a few extensions, to the corresponding headings in Table V. The J_i^π (possible) values entered in this Table are simply those for which the fits to the angular-distribution data satisfied the 1.0% criterion of the χ^2 test. As mentioned above, there is usually a multiplicity of values satisfying this condition. The entries in the δ column correspond to the minima in the χ^2 curves, and the upper and lower bounds on each value represent the intercepts of the χ^2 curves with the 1% probability lines. Whenever $\delta=0$ satisfied the 1% criterion, zero mixing was taken as the lower limit. In the few cases for which the χ^2 curve dipped below the 1% line more than once, only the particular set of values most relevant to a discrimination between possible spins was entered. The transition strengths listed are computed from the measured values of $g\Gamma_\gamma$, the assumed spin, and the corresponding value of δ.

The selection of the spin-parity combinations entered under the column heading J_i^π (preferred) was determined largely by the information included in the rest of the table. Occasionally, reference to the detailed information contained in Fig. 6 was needed in order to resolve borderline cases. To discriminate among the various values of J_i^π(possible) for a given level, the tabulated transition strengths for the designated multipole orders were compared with the empirically established ranges of values for these strengths. The acceptable ranges (in Weisskopf units) for the multipole orders of interest were taken to be[18] $M1\leq1$, $E2\leq100$, $M2\leq2$, $E3\leq20$, $M3\leq100$. For each row of the Table, the transition strengths were calculated for different values of J^π and the corresponding tabulated values of δ. The value of J^π was entered without parentheses whenever the strengths for both multipoles fell within the accepted ranges. The value was also entered without parentheses if transition strengths within the accepted ranges can be obtained with values of δ which, though not giving the best fit to the angular-distribution data, correspond to fits satisfying a 10% probability criterion under the χ^2 test. Possible J_i^π values are excluded from the preferred list if transition strengths in the accepted range could not be obtained with values of δ for which the fits to the angular distribution satisfied the 1% criterion. Marginal cases, in which a spin-parity combination requires mixing values to satisfy requirements on transition strengths such that the angular distributions can be fitted with a low probability, are entered in parentheses.

[18] D. H. Wilkinson, in *Nuclear Spectroscopy*, edited by F. Ajzenberg-Selove (Academic Press Inc., New York, 1960); E. K. Warburton, Natl. Acad. Sci.—Natl. Res. Council, Publ. No. 474 (1962). N. B. Gove, in *Nuclear Spin-Parity Assignments*, edited by N. B. Gove and R. L. Robinson (Academic Press Inc., New York, 1966).

Owing to the incompleteness of the information available on the 12 states listed in this Table, single values for J_i^π (preferred) can be assigned in only three cases. For six states, two values must be entered, and for the remainder, the data are compatible with three or more of the J_i^π values listed as possible.

In summary, the analysis of the data catalogued in Tables IV and V leads to specific assignments of J_i^π (preferred) for 13 of the 26 states listed. The multipolarity of the radiation emitted in transitions from 17 of these states to the ground state is also identified. In all cases, the character of the radiation is either $E1$, $E2$, or $M1+E2$. Such a result is not unexpected in as much as ground-state transitions of higher multipolarities would ordinarily be unable to compete successfully with those of lower multipolarities going to intermediate states.

7. TRANSITION STRENGTHS

Apart from their role in determining J^π assignments, the transition strengths merit attention in their own right in those instances in which the multipolarity of the radiation is definitely established. In particular, it is of interest to examine these data for evidence of features that might either be correlated with known properties of the level structure of Sc^{41} or draw attention to new aspects of that structure. Consider therefore the transition strengths associated with the multipoles for which the experimental data are most abundant, namely $E1$ and $E2$.

A. $E1$ Transitions

Seven transitions are identified as being predominantly electric dipole in character. If the weak $M2$ admixture, which may be present in some cases, is ignored, the $E1$ transition strengths derived from the data fall mostly in the range 10^{-3}–10^{-4} Weisskopf units. Six of these transitions originate in states for which $J^\pi=\frac{5}{2}^+$. Their average strength is 5.6×10^{-4} W.u. The average deviation of individual values is 2.8×10^{-4} W.u. The strengths of these transitions fall well within the range defined by known $E1$ transitions of this energy in nuclei in the mass-40 region. Indeed, in Bartholomew's compilation[19] of data on $E1$ transitions resulting from neutron capture, the 12 cases relevant to this discussion have an average strength of 4.6×10^{-4} W.u. The seventh transition originates in a state with $J^\pi=\frac{9}{2}^+$. Its strength is 3.2×10^{-3} W.u. after correcting for a small $M2$ admixture. This value is the largest $E1$ transition strength found in either the present body of data or that examined by Bartholomew. In this connection, it is possibly of interest to note that this state has a proton reduced width γ_p^2 of about 5% of the single-particle limit $\frac{3}{2}(\hbar^2/ma^2)$. This is about 16 times the average

[19] G. A. Bartholomew, Natl. Acad. Sci.—Natl. Res. Council, Publ. No. 974 (1962).

TABLE VI. Comparison between the reduced transition probabilities $B(E2;J_n\to J_0)$ and the limit imposed by sum rule.[a]

Transition energy (MeV)	J_n^π	$B(E2;J_n\to J_0)$ e^2 (fm)^4	$B(E2;J_n\to J_0)$ / $(E_{J_n}-E_{J_0})(2J_n+1)$ (sum) e^2
1.714	$\frac{3}{2}^-$	109.5	9.1×10^{-3}
2.584	$\frac{5}{2}^-$	27.0	5.1×10^{-3}
4.018	$\frac{7}{2}^-$	10.4	4.1×10^{-3}
4.950	$\frac{5}{2}^-$	2.2	$[0.8\times10^{-3}]$
		35.3	$[12.7\times10^{-3}]$
5.008	$\frac{7}{2}^-$	20.3	9.8×10^{-3}
5.140	$\frac{3}{2}^-$	1.7	0.4×10^{-3}
5.856	$\frac{3}{2}^-$	6.6	1.9×10^{-3}
			Total 3.1×10^{-2} or 4.3×10^{-2}
			$J_n^\pi=\frac{5}{2}^-$ $J_n^\pi=\frac{7}{2}^-$
5.650	$\frac{5}{2}^-,\frac{7}{2}^-$	7.6	3.1×10^{-3} 4.2×10^{-3}
5.706	$\frac{5}{2}^-,\frac{7}{2}^-$	28.2	11.7×10^{-3} 15.7×10^{-3}
5.868	$\frac{5}{2}^-,\frac{7}{2}^-$	24.0	10.3×10^{-3} 13.7×10^{-3}
5.970	$\frac{5}{2}^-,\frac{7}{2}^-$	6.5	2.8×10^{-3} 3.8×10^{-3}
			Total 2.8×10^{-2} or 3.7×10^{-2}

[a] The term "sum" in the denominator of the fraction in the heading of Column 4 stands for $(2J_0+1)[(25\hbar^2A/16\pi M)\langle r^2\rangle]$.

value of reduced widths found for the six $J^\pi=\frac{5}{2}^+$ states under consideration.[2]

B. *E2* Transitions

Of the 26 transitions for which data are listed in Tables IV and V, ten involve the emission of either pure $E2$ or mixed $M1$ and $E2$ radiation. In each case, the transition strength $|M(E2)|^2$ falls within a factor of 4 of the single-particle (Weisskopf) estimate. One other definite $E2$ transition, not included in these Tables, has a strength of 13 W.u. It originates in the first excited state of Sc^{41}, at 1.71 MeV, for which $J^\pi=\frac{3}{2}^-$. This transition has been discussed previously in detail by Youngblood *et al.*[20]

It is customary to express the transition strengths in single-particle units since this makes them directly applicable in choosing the values of J^π for the radiating states, as discussed in Sec. 6. Aside from this practical benefit, transition strengths so expressed are chiefly of value in furnishing evidence as to whether or not collective nuclear motion occurs in the states being scrutinized. Such motion is well known to be correlated with transition strengths substantially enhanced over the single-particle value.

With respect to the present body of data, it is seen that the evidence for collective motion is negligible except in the case of the 1.71-MeV state whose transition strength is enhanced by a factor of 13. However, even for this state the evidence is not decisive since the enhancement factor is not large, and moreover is sensitive to the magnitude of the single-particle unit (a quantity which, being model-dependent, is an inexact gauge of enhancement). Indeed, more refined estimates of the magnitude of the unit[21] can reduce the stated enhancement of the 1.71-MeV transition by as much as a factor of 6.

In seeking a firmer basis for characterizing transition strengths, one has recourse to the theoretical limits provided by sum rules. Among the sums that may be considered, the energy-weighted sum

$$\sum (E_n-E_0)B_n(EL)/e^2$$

is the most useful since the corresponding theoretical limit depends primarily upon the nuclear charge distribution in the ground state; and this distribution is known from electron scattering data.[22] For $E2$ transitions for which the change in isotopic spin is $\Delta T=0$, as in the present case (the first $T=\frac{3}{2}$ state[23] is at 5.9 MeV), the sum rule[24] is

$$\sum_{J_n}(E_{J_n}-E_{J_0})(2J_n+1)B(E2;J_n\to J_0)/e^2 = (2J_0+1)[(25\hbar^2A/16\pi M)\langle r^2\rangle],$$

where e is the electron charge, A is the mass number of the radiating nucleus, M is the nucleon mass, $\langle r^2\rangle$ is the second moment of the nuclear charge distribution and $(E_{J_n}-E_{J_0})$ is the transition energy between the nth energy level of spin J_n and the ground state of spin J_0. $B(E2;J_n\to J_0)$ is the reduced transition probability for $E2$ radiation from the nth level. For comparison with the sum rule, the transition strength of the nth level is specified by the ratio of the J_nth term in the sum to the theoretical limit of the sum. $B(E2)$ is related to the experimentally determined radiation width $\Gamma_\gamma(E2)$ in eV by the formula

$$\Gamma_\gamma(E2)=2.385(E/19.7)^5B(E2;J_n\to J_0)/e^2,$$

where E is the transition energy in MeV.

The data for the 11 transitions being considered in this section, when treated by means of the foregoing expressions, furnish the values of $B(E2;J_n\to J_0)/e^2$ and of transition strengths listed in Table VI. The transition strengths are based upon a theoretical limit for the sum computed to be 82.4×10^3 MeV fm^4 when the value of $\langle r^2\rangle$ given by Hofstader[25] for Ca^{40} is used. In the upper portion of the table are grouped the results for seven transitions originating in states for which J^π is known and for which the mixing ratio δ is also available when the transition involves an $M1$ and $E2$ mixture. In the case of the 4.950-MeV transition, a double root for

[20] D. H. Youngblood, J. P. Aldridge, and C. M. Class, Phys. Letters **18**, 291 (1965).

[21] P. P. Singh, R. E. Segel, R. H. Siemssen, S. Baker, and A. E. Blaugrund, Phys. Rev. **158**, 1063 (1967).

[22] A. M. Lane and E. D. Pendlebury, Nucl. Phys. **15**, 39 (1960); A. M. Lane, *Nuclear Theory* (W. A. Benjamin, Inc., New York, 1964), p. 80; O. Nathan and S. G. Nilsson, in *Alpha-, Beta-, and Gamma-Ray Spectroscopy*, edited by Kai Siegbahn (North-Holland Publishing Co., Amsterdam, 1965), Vol. I, p. 601.

[23] A. M. Poskanzer, R. McPherson, R. A. Esterlund, and P. L. Reeder, Phys. Rev. **152**, 995 (1966).

[24] D. Kurath (private communication).

[25] R. Hofstader, Ann. Rev. Nucl. Sci. **7**, 231 (1957).

TABLE VII. Energies and values of J^π of states in Sc^{41}.

Excitation energy (MeV) (p,γ)	(p,p)[a]	l_p[a]	J^π	J^π (provisional)	E_{exc} (calculated)[b] (MeV)	J^π[b]
1.714[c]			$\frac{3}{2}^-$			
	[2.094][d]	2	$\frac{3}{2}^+$		2.100	$\frac{3}{2}^+$
	2.409[c]	1	$\frac{3}{2}^-$			
2.584			$\frac{5}{2}^-$		2.529	$\frac{5}{2}^+$
2.663			$\frac{5}{2}^\pm,\frac{9}{2}^+$			
	2.713	0	$\frac{1}{2}^+$			
2.879			$\frac{7}{2}^-(\frac{7}{2}^+,\frac{5}{2}^-)$			
2.969			$\frac{7}{2}^-(\frac{7}{2}^+)$		2.977	$\frac{1}{2}^+$
3.182			$\frac{5}{2}^-,\frac{9}{2}^+$			
	3.411	0	$\frac{1}{2}^+$			
	3.467[c]	1	$\frac{1}{2}^-$		3.549	$\frac{9}{2}^+$
3.675					3.591	$\frac{7}{2}^+$
3.692			$\frac{5}{2}^-,\frac{7}{2}^\pm$			
	3.729	1		$\frac{1}{2}^-$		
	3.769	1		$\frac{1}{2}^-$		
3.778	3.779	2	$\frac{5}{2}^+$			
	3.966	0	$\frac{1}{2}^+$			
4.018			$\frac{7}{2}^-$			
4.027			$\frac{5}{2}^-,\frac{7}{2}^\pm$			
4.242	4.244	2	$\frac{5}{2}^+$		4.248	$\frac{11}{2}^+$
4.325						
4.437			$\frac{3}{2}^-,\frac{5}{2}^{(\pm)},\frac{7}{2}^{(\pm)}$			
	4.501	2		$\frac{3}{2}^+$		
4.511			$\frac{5}{2}^-,\frac{9}{2}^+$			
	4.532	1		$\frac{3}{2}^-$		
	4.639	1		$\frac{1}{2}^-$		
	4.774	2		$\frac{3}{2}^+$		
4.808			$\frac{5}{2}^-,(\frac{7}{2}^-),\frac{9}{2}^+$			
4.868	4.864	2	$\frac{5}{2}^+$			
	4.944	2		$\frac{3}{2}^+$		
4.950	4.947	3	$\frac{5}{2}^-$			
5.008			$\frac{7}{2}^-$			
	5.019	0	$\frac{1}{2}^+$			
5.036	5.031	4	$\frac{9}{2}^+$		5.043	$\frac{3}{2}^+$
	5.067	1		$\frac{1}{2}^-$		
	5.078	2		$\frac{3}{2}^+$	5.083	$\frac{15}{2}^+$
5.140	5.139	1	$\frac{3}{2}^-$			
5.164						
5.197						
5.222						
5.321						
	5.353	2		$\frac{3}{2}^+$		
5.376	5.371	2	$\frac{5}{2}^+$			
	5.392	1		$\frac{1}{2}^-$		
	5.416	2		$\frac{5}{2}^+$[a]		
	5.490	1		$\frac{1}{2}^-$		
	5.490	0	$\frac{1}{2}^+$			
5.521	5.516	2,3,4		$\geq\frac{5}{2}^\pm$		
	5.530	1		$\frac{3}{2}^-$[a]		
5.534						
5.565						
5.571	5.571	2	$\frac{5}{2}^+$		5.611	$\frac{13}{2}^+$
5.650	5.648	3	$\frac{5}{2}^-,\frac{7}{2}^-$			
5.690	5.690	2,3,4		$\geq\frac{5}{2}^\pm$		
	5.698	1		$\frac{1}{2}^-$		
5.706	5.703	3	$\frac{5}{2}^-,\frac{7}{2}^-$			
5.713					5.730	$\frac{5}{2}^+$
	5.755	1		$\frac{1}{2}^-$		
5.776						

TABLE VII. (*Continued*).

Excitation energy (MeV) (p,γ)	(p,p)[a]	l_p[a]	J^π	J^π (provisional)	E_{exc} (calculated)[b] (MeV)	J^π[b]
5.798	5.796	2,3,4		$\geq\frac{5}{2}^\pm$		
5.813						
	5.834	2		$\frac{3}{2}^+$		
5.856	5.857	1	$\frac{3}{2}^-$			
	5.861	2		$\frac{3}{2}^+$		
5.868	5.866	3	$\frac{5}{2}^-,\frac{7}{2}^-$			
5.912						
5.970	5.967	3	$\frac{5}{2}^-,\frac{7}{2}^-$			
	5.983	1		$\frac{3}{2}^-$[e]		
	6.013	0	$\frac{1}{2}^+$			
	6.045	1		$\frac{3}{2}^-$[e]		
6.055						
6.083						
6.109						
6.113						
	6.126	2		$\frac{3}{2}^+$		
6.145	6.141	2	$\frac{5}{2}^+$			
					6.202	$\frac{11}{2}^+$

[a] Reference 2.
[b] Reference 27.
[e] State also observed with $Ca^{40}(d,n)Sc^{41}$ and $Ca^{40}(He^3,\alpha)Sc^{41}$ reactions (Ref. 1).
[d] State observed only with the $Ca^{40}(He^3,d)Sc^{41}$ reaction (Ref. 1).
[e] Reference 26.

δ occasions the entry of two values of $B(E2)$. In the lower portion of the Table are grouped the results on four transitions originating in states whose spins in each case may be either $\frac{5}{2}$ or $\frac{7}{2}$, but for which values of δ are not known. The listed values of $B(E2)$ were estimated in each case by first averaging the values of Γ_γ corresponding to these spins and then computing the intensity of the $E2$ component on the assumption that $\delta^2=1$. This value of δ^2 is approximately the average of those found for the four transitions of like spin listed in the upper part of the table. It is believed that the results so derived should be fairly indicative of the actual magnitudes of the $E2$ transition strengths in these cases.

Inspection of the results listed in the right-hand column of the Table shows that the strength of individual transitions is typically 1% or less of the limit established by the sum rule. Furthermore, no one transition is seen to be distinguished from the others by exceptional strength; the value of the 1.71-MeV transition, in particular, is well within the range defined by the other cases. It is also seen that the combined strengths of the 11 transitions exhaust only 6–8% of the sum. However, this value does not include the contributions from some known states that still have not been identified as emitters of $E2$ radiation. But the number of these states can be estimated; and by using an average value of transition strength, the approximate magnitude of the missing component of transition strength can be computed.

The most likely sources of this missing $E2$ strength are the states that are listed in Table I without assigned values of J^π. There are 27 such states but only those of odd parity are allowed to emit $E2$ radiation in transitions to the ground state. The fraction in this category can be estimated from evidence furnished by states of known parity. Of 88 such states listed by Brown *et al.*,[2] one-half have odd parity. Of 18 states listed in Tables IV and V, 11 have odd parity. The evidence thus indicates that between one-half and two-thirds of the states in the group of 27 candidates probably would have odd parity and hence contribute $E2$ transition strength to the sum.

The average transition strength to be used in the computation can be estimated conservatively by use of the minimum values totaled for each group of transitions in Table VI. It is found to be 0.5% of the sum-rule limit. The product of this value and the number of transitions expected to originate in odd-parity states gives the desired estimate of the magnitude of the missing $E2$ transition strength. It amounts to 6–9% of the sum-rule limit.

When the estimated transition strength is combined with that totaled for the 11 transitions listed in Table VI 12–18% of the sum-rule limit is exhausted. To put these results in perspective, the transitions from the first 2^+ state to the ground state in even-even nuclei exhaust on the order of 10% of the sum, irrespective of the region of the periodic table examined. For Ca^{40} in particular, transitions from 2^+ states at 3.94 and 7.1 MeV together exhaust about 16% of the sum, of which 4% is contributed by the transition of lower energy.[22] It is evident that the $E2$ transition strength exhibited by Sc^{41}, although shared by a substantial number of states, is consistent in magnitude with that found in Ca^{40} and is distributed over a similar range of energy.

8. ENERGY LEVELS OF Sc^{41}

The energies and values of J^π of all known excited states of Sc^{41} occurring at energies up to 6.15 MeV are listed in Table VII. These data are drawn chiefly from the present work and the earlier studies of proton elastic scattering. The energies of 76 states are listed in the Table in one or both of the columns headed $E(p,\gamma)$ and $E(p,p)$ according to the source of the data for each entry. Inspection of the entries shows that 29 states are observed only by the (p,γ) reaction and a like number only by the (p,p) reaction. Seventeen states are seen to be common to both reactions, levels being so classified if their energies agree to within 5 keV. Despite such agreement in energy, separate states are indicated for the entries of 5.530 and 5.534 MeV in the (p,p) and (p,γ) columns, respectively; there is evidence that the widths measured for resonances at these energies in the two experiments are substantially different. The 2.094-MeV level in the $E(p,p)$ column is entered in brackets to indicate that this state is seen only with the $Ca^{40}(He^3,d)Sc^{41}$ reaction.[1]

The fourth column of the Table lists values of J^π for 36 states for which the evidence bearing on spin assignments is most conclusive. Of the entires in this column, 26 are J^π (preferred) assignments given in Tables IV and V. The assignment $J^\pi=\frac{3}{2}^-$ for the state at 1.714 MeV is the value previously assigned by Youngblood.[20] The 9 remaining entries involve states not previously discussed in this report but for which assignments are available because of some special circumstances. Assignments of $J^\pi=\frac{1}{2}^+$ follow immediately for six states exhibiting s-wave resonances in the proton scattering data. The state listed at 3.467 MeV is assigned $J^\pi=\frac{1}{2}^-$ on the basis of an analysis of a p-wave scattering resonance at this energy; it distinguishes the value of J in this case because the resonance is exceptionally broad.[2] The two final entries $J^\pi=\frac{3}{2}^+$ and $\frac{3}{2}^-$ for the states at 2.094 and 2.409 MeV, respectively, were assigned by analogy with states of these spins and otherwise quite similar spectroscopic properties[1] located at 2.017 and 2.471 MeV in Ca^{41}.

The fifth column of the Table lists provisional values of J^π for 24 states which are observed in the (p,p) but not in the (p,γ) reaction. In all cases, the states are excited by either p- or d-wave scattering. These features imply assignments of either $J^\pi=\frac{3}{2}^+$ or $\frac{1}{2}^-$ for these states since, for either value, the multipolarity of the radiation emitted in the transition to the ground state would be sufficiently high to make the transition improbable in competition with more favorable modes of radiative decay. Accordingly, unless there is other evidence to the contrary, one or the other of these values is listed for each state, depending upon the partial wave involved in the scattering process. However, in several cases associated with p-wave resonances, an assignment $J^\pi=\frac{3}{2}^-$ has been entered because this value is either favored by the analysis of the elastic scattering data or is required by the results of angular-distribution studies of the protons inelastically scattered at the energies of these resonances.[26]

For comparison with the experimental data, the two final columns of the Table list the energies and spins of positive-parity states of two-particle–one-hole character that are predicted by the shell-model calculations recently reported by Armigliato *et al.*[27]

[26] N. A. Brown (private communication).

[27] A. Armigliato, L. M. El-Nadi, and F. Pellegrini, Nuovo Cimento **49B**, 142 (1967).